Spectro-polarimetric signature of a random laser

Sebastian Knitter,* Michael Kues, and Carsten Fallnich
Institut für Angewandte Physik, Westfälische Wilhelms-Universität, Corrensstraβe 2, 48149 Münster, Germany
(Received 29 April 2013; published 24 July 2013)

We characterized the spectro-polarimetric emission properties of random lasers in the regime of strong scattering. The study involved the preparation of microstructured samples, which were shown to support very stable random laser modes in spectral location and intensity. We show that random lasing modes from such samples are highly polarized in statically random, but well-defined states that can be used as a unique sample identifier. Our findings reveal a strong dependency of the emission spectrum on the pump polarization and demonstrate how the spectro-polarimetric emission can be efficiently manipulated.

DOI: 10.1103/PhysRevA.88.013839 PACS number(s): 42.55.Zz, 42.25.Fx, 42.25.Ja

I. INTRODUCTION

When optical amplification in a scattering medium compensates the diffusive losses, coherent *random lasing* (RL) modes may occur. After exceeding a certain pump threshold intensity, these are most often characterized by narrow peaks in the emission spectrum, very much reminiscent of modes in a conventional laser. This process was observed in many different materials and mainly characterized by the spatial, spectral, and temporal emission profile. Extensive review on the matter can be found in [1–3] and the references therein.

To date only liquid dye-based random lasers in the diffusive regime of weak scattering (inverse optical turbidity $kl_t > 100$) were characterized by their spectro-polarimetric emission properties [4]. This study showed that the anisotropic absorption of the incorporated laser dye dominated the polarization of the RL modes. The operational principle of these systems is closely related to a Fabry-Pérot–like feedback mechanism between the entrance face of the sample container and particles on the other end of the gain volume [5]. Due to the mobility of the TiO_2 scatterers in the solution, the boundary conditions for RL modes changed greatly from pump pulse to pump pulse. As a result the samples emitted spectra with high variability.

Another class of random lasers exists in the strong-scattering regime ($kl_t \ll 100$), which was investigated in this study. These samples usually consist of strongly scattering particles, with the capacity to amplify light. Here the emission spectrum is independent of feedback from the sample interfaces and is solely defined by the interplay of multiple scattering and gain in the random structure. The advantages of these "dry" random lasers, made from crystalline materials, are the stable emission spectrum and the low photodegradation. As shown in [6,7], it is possible to construct these lasers in microscopic volumes, which is also our preferred method of preparation.

It has been shown that the spectral location of RL peaks in statically random samples is also random but determined by the nanoscopic structure of the scattering medium [8]. With our detection technique it is now also possible to characterize the polarization of these RL modes individually [9], a widely uncharted area of the field. In this article we present measurements on the polarization of RL modes in strongly scattering media. First, we present our approach to manufacture a microscopic random laser (MRL), with very high spectral stability and a recognizable emission spectrum. Second, we show that the polarization states of these modes are distributed randomly and are strongly dependent on the pump polarization. Possible applications arise due to these properties by using the random laser's unique spectro-polarimetric signature, e.g., as a marker in anticounterfeiting applications. The measurements presented in the following sections are meant as examples, illustrating the generally observed behavior.

II. METHODS

All random lasers were excited with pulses from a diode-pumped Nd:YAG-laser ($\lambda = 355\,\text{nm}$, $\tau_{\text{pulse}} = 50\,\text{ps}$, $\nu_{\text{rep}} = 10\,\text{Hz}$). Figure 1 illustrates how pump light was fed into the collinear pumping and detection scheme with a glass-wedge beam splitter (BS) and focused onto the sample with a UV-optimized microscope objective (MO, $f_{\text{EFL}} = 13\,\text{mm}$, NA = 0.32). The emission from the sample was collected with the same microscope objective and fed into a spectro-polarimeter, which due to the low emission intensity of ZnO, had to be slightly modified from the original setup [9]. Rather than illuminating the static modulator-crystal (MC) at the entrance slit of a monochromator along the vertical, the light was focused onto the entrance slit and modulated with a vertically moving modulator crystal in a prefocus. With the conventional method [9] the light would have been vertically dispersed and distributed over 100 pixel rows, which would have resulted in a 100 times smaller signal (per pixel row) with readout noise for each of the 100 pixel rows. In the variation used for this study, we imaged the sample onto the entrance slit of the monochromator, binned all vertical pixels together, and essentially read only one horizontal line of the CCD sensor, with the according readout noise of only one line. This procedure allowed improvement of the signal-to-noise ratio of the assembled polarigram by about 2 orders of magnitude to the expense of the single-shot acquisition capability compared to the initial setup. The polarigram was assembled later for 100 different positions of the modulator crystal and used for the reconstruction of polarization states by use of a calibration [10]. The calibration was verified by feeding actual RL emission through a polarizer and into the polarimeter. It was checked that the measured linear polarization agreed with the prediction at the polarizer angle from 0 to 180° in steps of

*Corresponding author: sebastian.knitter@uni-muenster.de

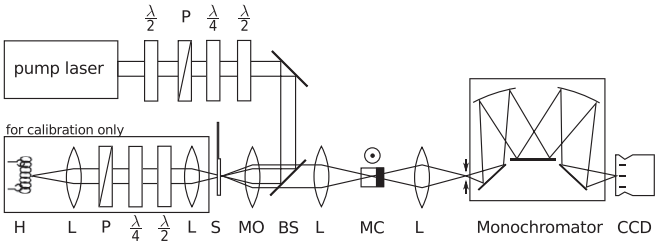

FIG. 1. Experimental setup - λ/4, λ/2: quarter-/half-wave plate; P: polarizer; BS: beam splitter; MO: 15× microscope objective; S: sample; L: lens; MC: modulator crystal; CCD: image sensor; H: halogen lamp. Components in the dotted region were used for the calibration of the apparatus, according to [9].

20°. As expected, the measured polarization state moved with the orientation of the polarizer and the degree of polarization $DoP = \sqrt{S_1^2 + S_2^2 + S_3^2}/S_0$ was close to unity.

III. MICROSCOPIC RANDOM LASERS

Comparable to [8], emission spectra from area-coated (AC) samples were similar for a series of successive pump pulses. The emission spectra were strongly dependent on the sample location, with a very high displacement sensitivity on the order of 100 nm. This is due to the comparable size of the central region of the pump spot, inverting the sample, with the surface roughness of the random medium. This displays a very strong demand on the required repositioning accuracy and is prohibitive for many real-world applications in which reproducible emission spectra are desired. Also the pulse-to-pulse fluctuations in the emission spectrum of these samples are usually high (>30%).

In order to solve this problem, we manufactured microscopic cavities in glass substrates by femtosecond laser ablation ($\varnothing = 5 \pm 2$ μm, conical depth profile pointing into the substrate), which were filled with nanoparticles from zinc oxide (Merck-Emprove, $\varnothing = 200$ nm) in wet, pasty ethanol dispersion. After the dispersion was applied to the substrate, the ethanol was left to evaporate. The remaining material was cast off with a razor blade, leaving the clean substrate surface and the MRL cavities. This procedure was repeated until all microcavities were sufficiently filled. Zinc oxide is a popular material for dry random lasers [6,7,11,12], as it is cheap, widely available, nontoxic, and well characterized [13,14].

The advantage of the MRL over the AC samples lies in the fact that the inverted region, in this case the entire sample, is strictly limited to the microcavity and not surrounded by other population-inverted nanoparticles. For the AC samples there is always a mode volume in the tail of the pump-spot profile that is close to the lasing threshold and thus shows large pulse-to-pulse fluctuations. These fluctuating modes interact with the main modes in the gain volume and lead to an intrinsically unstable emission spectrum. Generally speaking, it is very difficult to attain constant spectra when the size of the pump spot is not sufficiently small. In order to attain the lowest possible pulse-to-pulse fluctuations, AC samples were pumped with small spot sizes, just above the threshold intensity ($\varnothing \approx 1$ μm, $E = 10$ nJ). The MRL samples, on the other hand, were pumped with a spot size larger than the MRL itself ($\varnothing \approx 10$ μm) to provide a homogeneous pump intensity across the entire sample, leading to the emission of highly stable and similar spectra.

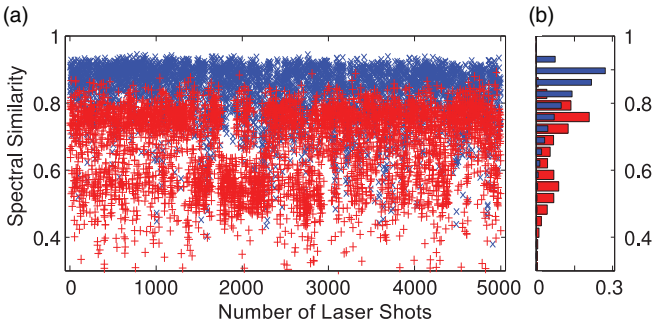

FIG. 2. (Color online) (a) Temporal evolution of the spectral similarity of spectra from AC samples (red-plus symbols) and MRL samples (blue-cross symbols) with respect to the average spectrum. Sim [Eq. (1)] is generally smaller for AC samples. (b) The area-normalized histogram of the two traces in (a) reveals two distinct classes of emission spectra, one that is more similar to the average spectrum and at least one that is different. Spectra from MRL are more similar to each other, with a peak similarity at 0.9.

To characterize the spectral similarity between two background-subtracted spectra $I_a(\lambda)$ and $I_b(\lambda)$, under different conditions, e.g., for different times $a = t_0$, $b = t$ or for a pump spot in different locations $a = x_0$, $b = x$ on the sample, we introduced the similarity parameter

$$\mathrm{Sim}(I_a(\lambda), I_b(\lambda)) = \frac{I_a(\lambda) \star I_b(\lambda)}{\sqrt{[I_a(\lambda) \star I_a(\lambda)][I_b(\lambda) \star I_b(\lambda)]}}, \quad (1)$$

with

$$I_a(\lambda) \star I_b(\lambda) = \int I_a(\lambda) I_b(\lambda) d\lambda. \quad (2)$$

Sim is zero if the peaks within the spectra $I_a(\lambda)$ and $I_b(\lambda)$ have no spectral overlap and 1 if both spectra are identical.

Figure 2(a) shows the time evolution of the spectral similarity Sim of 5000 consecutive emission spectra and their average spectrum. This measurement indicates how reproducible emission spectra from different sample types (AC/MRL) are, if all other conditions remain the same. While Sim is rather constant for MRL (blue trace), it is lower and more strongly fluctuating for AC samples. A histogram analysis of this data [Fig. 2(b)] shows how the distribution of modes from the MRL peaks at about 0.9 (blue trace), while the AC samples have two peaks at 0.55 and 0.75 (red trace). These maxima indicate that the AC samples emitted a superposition of at least two different spectra, both of which carry significant differences to the average spectrum. Spectra emitted from MRL, on the other hand, are very similar to each other.

Another advantage of the MRLs is the reduced susceptance to small sample displacements ($x_0 \rightarrow x$) and angular pump-beam jitter, when pumped with a laser spot much larger than the sample itself. The similarity between the emission spectrum at different sample positions x is compared to emission spectra at a reference point x_0 in Fig. 3. This displacement scan indicates how well random lasers of different kinds (AC/MRL) have to be repositioned in order to recognize particular samples by

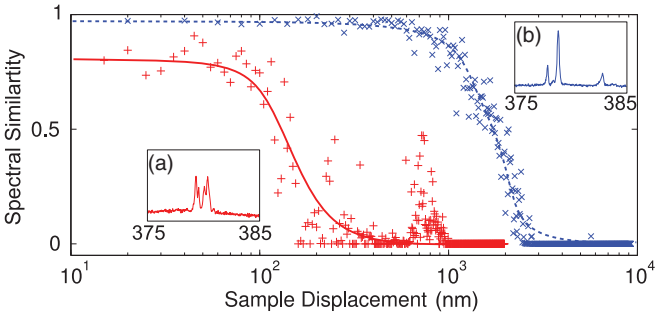

FIG. 3. (Color online) MRL samples (blue-cross symbols) display a much higher spectral similarity over a 1 order of magnitude larger displacement compared to AC systems (red-plus symbols). Red-full and blue-dotted lines guide the eye. The insets (a) and (b) show example spectra of the corresponding sample types.

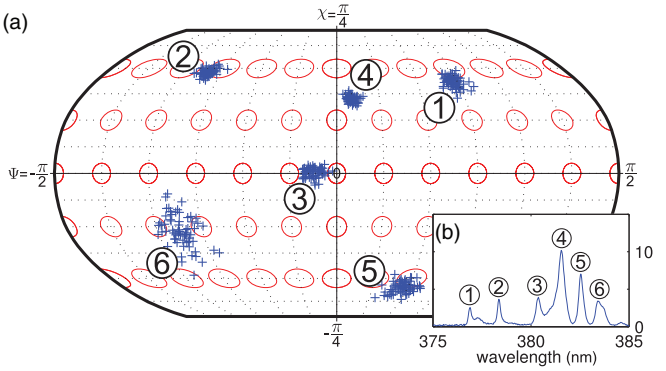

FIG. 4. (Color online) (a) Six RL modes in 60 successive measurements plotted on the Poincaré sphere in cartographic Robinson projection [15]. Red Tissot indicatrices (ellipses) illustrate the distortion. (b) The inset shows an example spectrum with numbered peaks.

their emission spectrum. For the MRL sample the similarity was much larger (>0.9) and extended over roughly 1 order of magnitude wider (>1 μm) than for AC samples (≈100 nm). Unexpectedly, the allowed sample displacement was still smaller than the diameter of the sample. We attribute this to the natural radial intensity variation of the Gaussian-shaped beam profile. An additional disadvantage of the requirement for low pump intensities in the AC case is the small amplification bandwidth, limiting the spectral range over which RL modes can exist. As depicted in Fig. 3(a), only few modes reach the threshold in a narrow spectral region. These spectra naturally appear similar due to the bandwidth limitations and cause the secondary Sim maximum in the red trace of Fig. 3.

In summary, MRL peaks are very stable, with a standard deviation of typically less than 0.3 nm in peak wavelength and about 10% in spectral peak intensity over 5000 pump-laser shots. They are well suited for the spectro-polarimetric characterizations of RL emission, where constant emission spectra are required.

IV. SPECTRO-POLARIMETRIC MEASUREMENTS

Not only were the spectral locations of RL modes constant, but also the polarization was reproduced excellently. When a MRL was pumped well above threshold, six distinguishable RL modes over a spectral range of about 7 nm were supported [Fig. 4(b)]. For 60 consecutive spectro-polarimetric measurements, the polarization properties of these modes were characterized. Results are depicted in Figs. 4(a) and 4(b), and peak properties such as intensity, degree of polarization (DoP), and their relative standard variations tabulated in Table I. Over the course of 6000 pump pulses, the sample degradation was insignificantly small, which is a great advantage over dye-based random lasers.

The polarization of the individual modes was localized within small areas of the Poincaré sphere ($\sigma_{\Psi\chi} < 0.1$ rad), which were not overlapping and distributed in different octants of the Poincaré space [Fig. 4(a)]. Out of all modes, mode ⑥ was the least stable. It displayed the largest spread in measured polarization states and also the largest intensity fluctuations. The deviation from the average of the 60 individual measurements constituting each point cloud in Fig. 4(a) was random, without an apparent pattern. A gradual sample deformation due to thermal or photoinduced damage can thus be neglected.

The DoP was elevated, generally above 0.6 (modes ①–⑤), but also as high as 0.9 (mode ④). Usually DoPs were lower for weak, unstable modes, which were either close to their threshold or partially overlapping with other modes spectrally. Our measurements raised the question of how the DoP of light, originating from a stimulated emission process, can be anything less than completely polarized. The origin of lowered DoPs can have several reasons: (1) Because every polarimeter needs a certain time to make the measurement, the result is always an average over the full emission time. If a mode should start in one polarization state and change this state later during emission, e.g., due to mode competition, the polarimeter would measure a mixture of both signals and indicate an effectively lowered degree of polarization. (2) As a spectro-polarimetric measurement was performed here, the peaks of certain modes might overlap in the emission spectrum. The result in the overlap region is a superposition of both polarization states, and as long as these modes are not coherently coupled, a lowered DoP will be the consequence. (3) Another source of lowered DoPs in our polarimeter is the fact that each polarization measurement consists of 100 completely independent intensity measurements for different positions of the modulator crystal. Pulse-to-pulse fluctuations in the spectro-polarimetric emission profile may directly lead to a diminished DoP, even if each single emission should be completely polarized. Such fluctuations can be generated by

TABLE I. Selected properties of RL modes over 60 successive, independent measurements. Bright peaks showed generally smaller intensity fluctuations. The DoP was not correlated with the intensity.

Mode no.	λ (nm)	$\overline{\psi}$ (rad)	$\overline{\chi}$ (rad)	$\overline{S_0}$ (arb.units)	$\frac{\sigma(S_0)}{S_0}$ (%)	$\overline{DoP}$	$\frac{\sigma(DoP)}{DoP}$ (%)
①	376.9	+0.77	+0.43	2.2	16	0.83	4
②	378.4	−0.88	+0.51	3.3	10	0.81	8
③	380.4	−0.15	+0.01	4.0	3	0.66	5
④	381.5	+0.08	+0.37	10.3	5	0.88	3
⑤	382.6	+0.50	−0.58	7.9	9	0.61	7
⑥	383.4	−0.93	−0.24	2.9	16	0.45	12

sources not at all related to the specimen, e.g., fluctuations in the pump laser. After all, a low DoP is indicative of changing mode properties during the measurement, emission, or both. Even if it is possible to reduce these influences, it remains very difficult to distinguish these effects in the current measurement scheme. Under these considerations it is calming to see that the DoPs of RL modes in zinc oxide are still significantly elevated compared to noncoherent emission processes, as it is usually the case for fluorescent or thermal emission [4].

The persistence and reproducibility of the spectro-polarimetric emission properties show that they are indeed a consequence of the statically disordered boundary conditions in the medium and are disturbed only (if at all) by the initial spontaneous emission or mode competition.

Within the scope of coherent light fields interfering in the presence of optical gain and scattering, there is the question of how the pump polarization would influence the creation of RL modes. The measurement was performed by using a half- and a quarter-waveplate to set the pump polarization to arbitrary states. The pump energy in the plane of the sample was kept constant, and all series were recorded in random order to minimize the impact of sample degradation or thermal drift.

Turning the pump polarization by 180° around the equator of the Poincaré sphere over a range from $\Psi = -\pi/2$ to $+\pi/2$ the emission spectrum changed dramatically [Fig. 5(a)]. One spectral mode existed only in a limited pump polarization range ($\lambda \approx 375$ nm, $\Psi < 0$) and was completely discriminated by the orthogonal pump polarization ($\Psi > 0$). Also the spectral location and intensity of the individual modes was slightly dependent on the pump polarization.

When the pump polarization was changed from left-handed to right-handed circular polarization [i.e., from $\chi = -\pi/4$ to $+\pi/4$, $\Psi = 0$, Fig. 5(b)], the peak locations changed with discontinuous jumps (at $\chi = \pm 0.3$ rad), symmetrically with respect to the handedness of the pump polarization. The polarization state of individual modes was constant for different pump polarization throughout their region of existence (not shown here). When the pump polarization changed from horizontally linear to circular, more light was deposited into the vertical component. This way modes could be stimulated that would not have been existent when pumped in the horizontal polarization. The trace at circular pump polarization ($\chi = \pm\pi/4$) in Fig. 5(b) displays one major mode at 375.7 nm and minor components at 377.0 and 379.7 nm. All these modes appeared in the scan of linear pump polarization. We attribute the presence of all these modes to the fact that we implicitly pumped in the horizontal and vertical polarization directions simultaneously with a circular pump polarization. Competition between the modes might have caused one to be much brighter, to the expense of the other modes' existence.

Similar experiments with a dye-based random laser in the diffusive regime have revealed that the asymmetric absorption momenta of the amplifier have dominated the response to different pump polarizations [4]. Zinc oxide, however, does not display this asymmetry. At room temperature, the absorption cross sections for radiation polarized parallel and orthogonal to the c axis of the uniaxial crystal differ by only less than three percent from the average value [16]. The symmetry of the particles' crystal structure and the randomness of their orientation leaves only one explanation for the observed

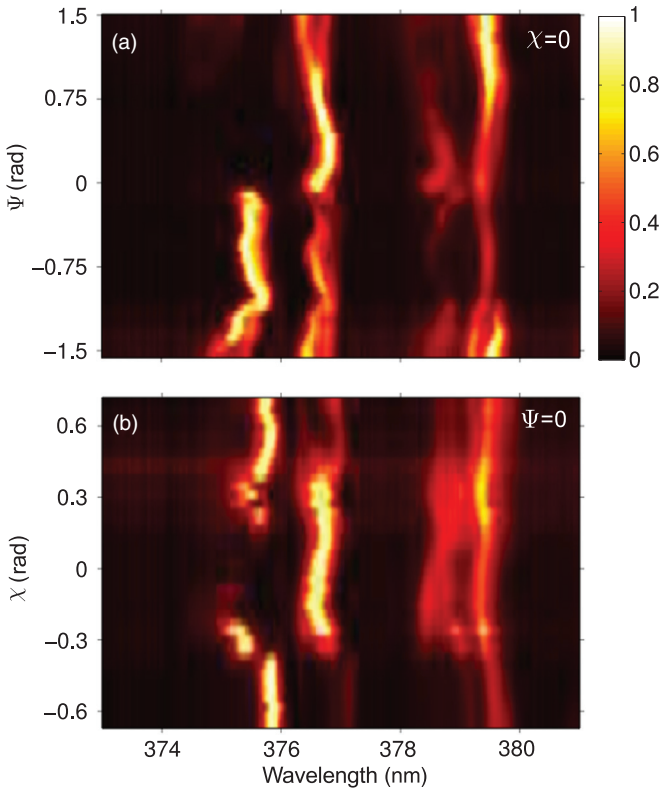

FIG. 5. (Color online) Color-coded spectral intensity of RL modes under different pump polarizations. Each spectral trace was mapped to the [0,1] interval to enhance visibility. The color bar applies to both graphs. (a) The linear pump polarization was turned by 180°. The dominant modes change their spectral location for different pump polarizations. (b) The pump polarization was scanned from left-handed circular to right-handed circular. Modes changed their spectral position with changing pump polarization, disregarding the handedness of the pump polarization.

behavior: As light scattering is generally polarization sensitive [17], the pump light will have a distinctive spatial profile inside the medium. Also, RL modes have a characteristic spatial structure [18] that is in turn dependent on their wavelength [19]. Apparently the overlap of the statically random, polarization-dependent spatial gain distribution with the spatial mode structure of the lasing modes couples the emission spectrum to the pump polarization. While modes can only exist when they have sufficient overlap with the pump mode, the existence of a lasing mode also changes the spatial inversion profile and in that way the pumping conditions for other modes. The close relation of the spatial pump profile, that in this case is altered by the pump polarization, and the RL mode's field distribution is currently perceived as an efficient method to control a random laser [20,21].

Because all these effects act simultaneously and can only be measured in an equilibrial state, it is impossible to separate them experimentally. In order to study the complicated and in general nonlinear interplay between pump polarization, spatial pump mode, laser modes, and laser-mode competition, three-dimensional numerical simulations similar to [19] would be necessary. In principle they can deliver the necessary means to observe the creation of RL modes with high temporal and spatial resolution of all important quantities (i.e., electric

field vectors and inversion), but are currently limited to very small media, due to their enormous memory requirements. We are presently developing such a simulation in order to investigate the coupling of spatial pump profile and spatio-spectral properties of RL modes.

V. CONCLUSION

In summary, we have shown how the preparation of a microscopic random laser increases the pulse-to-pulse emission stability and reduces the requirements for a sample realignment. The spectro-polarimetric emission properties from such miniaturized random lasers in the strongly scattering regime were characterized. RL modes occupy distinct polarization states at distinct optical frequencies that can be used as an identifier, which is unique to any given random laser. By exclusion of other explanations, RL modes and their polarization appear to be determined by interference of pump waves in the medium overlapping with the spatially random distribution of RL mode fields. By altering the pump polarization, certain peaks can be stimulated or completely discriminated. With this mechanism it is possible to manipulate the emission spectrum of optically pumped random lasers.

Zinc oxide, the material used in these experiments, was chosen for its proven support of RL modes but poses quite strong requirements on the pumping and detection hardware. For a real-world application of random lasers as markers, other materials must be identified that emit more brightly, in a more detector-friendly wavelength range, and with the potential to be pumped with a simpler and more cost-effective light source, e.g., a diode laser. Nevertheless, the measurements presented here show the great potential of the RL mechanism for a truly random sample identifier that is incredibly cheap and easy to manufacture—the "fingerprint" of a random laser.

ACKNOWLEDGMENTS

This work was supported by the German Federal Ministry of Education and Research (BMBF) within the compound project PEARLS under Grant No. 13N10154. We thank F. Korte and J. Kirschbaum from Micreon GmbH for the preparation of the microstructured substrates.

[1] H. Cao, J. Phys. A: Math. General **38**, 10497 (2005).
[2] M. Noginov, *Solid-State Random Lasers*, Springer Series in Optical Sciences (Springer, New York, 2005).
[3] D. S. Wiersma, Nat. Phys. **4**, 359 (2008).
[4] S. Knitter, M. Kues, and C. Fallnich, Opt. Lett. **37**, 3621 (2012).
[5] X. Wu, W. Fang, A. Yamilov, A. A. Chabanov, A. A. Asatryan, L. C. Botten, and H. Cao, Phys. Rev. A **74**, 053812 (2006).
[6] H. Cao, J. Y. Xu, E. W. Seelig, and R. P. H. Chang, Appl. Phys. Lett. **76**, 2997 (2000).
[7] J. Fallert, R. J. B. Dietz, J. Sartor, D. Schneider, C. Klingshirn, and H. Kalt, Nat. Photonics **3**, 279 (2009).
[8] K. L. van der Molen, R. W. Tjerkstra, A. P. Mosk, and A. Lagendijk, Phys. Rev. Lett. **98**, 143901 (2007).
[9] S. Knitter, T. Hellwig, M. Kues, and C. Fallnich, Opt. Lett. **36**, 3048 (2011).
[10] R. M. A. Azzam and A. G. Lopez, J. Opt. Soc. Am. A **6**, 1513 (1989).
[11] R. Thareja and A. Mitra, Appl. Phys. B **71**, 181 (2000).
[12] E. V. Chelnokov, N. Bityurin, I. Ozerov, and W. Marine, Appl. Phys. Lett. **89**, 171119 (2006).
[13] A. B. Djurišić and Y. H. Leung, Small **2**, 944 (2006).
[14] C. Klingshirn, B. Meyer, and A. Waag, *Zinc Oxide: From Fundamental Properties Towards Novel Applications*, Springer Series in Materials Science Vol. 120 (Springer, Berlin, 2010).
[15] A. H. Robinson, International Yearbook of Cartography **14**, 145 (1974).
[16] W. Y. Liang and A. D. Yoffe, Phys. Rev. Lett. **20**, 59 (1968).
[17] H. van de Hulst, *Light Scattering by Small Particles*, Structure of Matter Series (Dover Publications, Inc., New York, 1957).
[18] J. Andreasen, A. A. Asatryan, L. C. Botten, M. A. Byrne, H. Cao, L. Ge, L. Labonté, P. Sebbah, A. D. Stone, H. E. Türeci, and C. Vanneste, Adv. Opt. Photon. **3**, 88 (2010).
[19] A. Ghasempour Ardakani, A. R. Bahrampour, S. M. Mahdavi, and M. Golshani Gharyeh Ali, Opt. Commun. **285**, 1314 (2012).
[20] M. Leonetti, C. Conti, and C. Lopez, Nat. Photonics **5**, 615 (2011).
[21] N. Bachelard, J. Andreasen, S. Gigan, and P. Sebbah, Phys. Rev. Lett. **109**, 033903 (2012).